INTERNATIONAL JOURNAL
FOR RESEARCH

IN APPLIED SCIENCE & ENGINEERING TECHNOLOGY

Effect of High Pressure on Structural and Optical Properties of ZnTe : A Density Functional Study

Dr. P. K. Saini

Department of Physics, Govt PG College, Hansi, Haryana (India) 125033

Abstract: We present ab initio calculations of structural and optical properties of ZnTe with zinc-blende and rock-salt type structures using the density functional method within the generalized-gradient approximation (GGA) approach. From the calculated values of ground state energy we have determined the lattice constant, bulk modulus, pressure derivative of bulk modulus and optical properties. The optical spectra have been performed for the energy range 0-14 eV, without including the spin orbit coupling at ambient and high pressure. Absorption, reflectivity and refractive index have been calculated from the imaginary part of the dielectric function. The obtained results are in good agreement with the available experimental data.
Keywords: Lattice constant, bulk modulus, structural properties, GGA, optical spectra

I. INTRODUCTION

The group II-VI, ZnS, ZnSe and ZnTe are the prototype for II-VI semiconductors and their cubic phases, which occur naturally as a mineral, have been the subject of intense investigation. Zinc chalcogenides in the cubic sphalerite structure are direct-gap semiconductors with an energy gap ranging from 2.3 eV (ZnTe) to 3.7 eV (ZnS)[1-3]. Recent interest under the high pressure behaviour of zinc chalcogenide has arisen in the context of high pressure investigations for strain effects in the super lattices [4-7]. By using diamond- anvil cell techniques, the effect of pressure on the direct optical gaps of ZnSe [8] and ZnTe [9] has been investigated for pressure covering the full stability range of the tetrahedral phases. Zinc chalcogenides ZnX (X=S, Se, Te) crystallizes in the zinc-blende(ZB) type structure at ambient pressure and NaCl type rocksalt (RS) structure at high pressure. Several other studies have also been reported about these materials in the literature [2,8-11]. However, most of the studies were carried out experimentally and there were smaller effort to understand the theoretical electronic structure and optical properties particularly under high pressure which is very important for better understanding for this class of materials.

This paper present detailed study for the structural, electronic and optical properties of ZnTe in ZB and RS structures using DFT based FP-LAPW (WIEN2k) methods both for ambient and high pressure phases. Apart from the ground state energies and structural properties, we have also reported various optical properties.

II. METHODOLOGY

The present calculations of structural, electronics and optical properties have been carried out with a self-consistent scheme by solving the Kohn-Sham equations, using a FL-LAPW method in the framework of the density functional theory (DFT), as implemented in the WIEN2K code [12]. In the calculations, the most recently version of Vienna package WIEN2k (2011) has been applied. The alternative base sets (APW+lo) is used inside the atomic spheres for chemically important *l*-orbitals (partial waves). For all the other partial waves the LAPW scheme is used [13-16]. In the present study, 3p, 3d, 4s orbitals of Zn and 5s, 5p, 5d of Te have been treated as valence states. Moreover, we employ the semi-relativistic approximation (no spin orbit effects included) whereas the core levels are treated fully relativistic [16]. The generalized gradient approximation (GGA) was used for the exchange-correlation potential [17-22]. The unit cell was divided into two regions. The spherical harmonic expansion was used inside the non-overlapping spheres of muffin-tin radius (R_{mt}) and the plane wave basis set was chosen in the interstitial region (IR) of the unit cell. The R_{mt} for Zn and Te were chosen in such a way that the spheres did not overlap with each other. For the total energy convergence, the basis functions in the interstitial (IR) were expanded up to $R_{mt} K_{max} = 7.0$ and inside the atomic spheres for the wave function, where R_{mt} is the smallest muffin-tin radius. For calculation of linear optical properties we have used 3000 k-points. Pressure is obtained by taking the volume derivative of the total energy and bulk modulus is calculated by the P-V diagram. Further the optical properties are obtained from frequency dependent dielectric function for which the imaginary part of dielectric tensor can be computed from the electronic band structure of ZnTe.

III. RESULTS AND DISCUSSION

A. Structural Properties

The calculated total energies (E) with in GGA as a function of volume (V) were used for determination of theoretical lattice constant and bulk modulus. The equilibrium lattice constant, bulk modulus and its pressure derivative are calculated by fitting the calculated total energy to the Murnaghan's equation of state (EOS) [23]. The variations of the calculated total energy with volume for ZnTe in zinc blende and rock-salt phases are shown in the Figures. 1 and 2, respectively. The calculated results for structure optimization of ZB phase and RS phase of ZnTe are summarized in the Table I along with the earlier reported experimental and theoretical results.
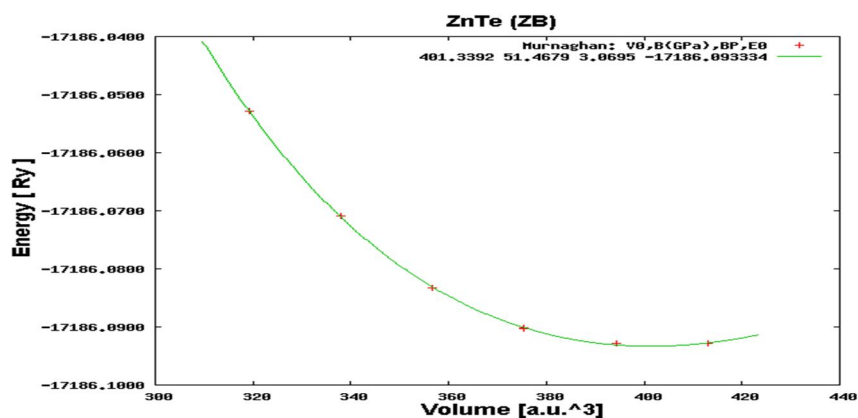

Figure 1: Energy vs volume for ZnTe in zincblende structure.

The calculated bulk modulus and its pressure derivative for B3 phase of ZnTe are 51.46 GPa and 3.06 respectively whereas the bulk modulus and its pressure derivative of high pressure RS phase of ZnTe are 52.53 GPa and 3.48, respectively. The optimized lattice constants of ZnTe is obtained as 6.18 Å for zinc blende phase whereas that is calculated as 5.78 Å for RS phase under the application of high pressure at about 14.88 GPa. At this high pressure ZnTe is found to be existing in RS phase in more stable form. When the results were compared with earlier reported values, it is found that these results are in good agreement with the earlier reported experimental results as compared to the earlier reported theoretical results by other methods [24-25]. However, still earlier reported experimental results are found slightly different from our calculated results which may be explained on the fact that GGA calculate bulk modulus always more than the experimental values, which is a general trend. This little difference may also be interpreted due to an another fact that the experimental values of the bulk modulus are somehow uncertain due to the difficulty of growing high-quality single crystals in the laboratories.
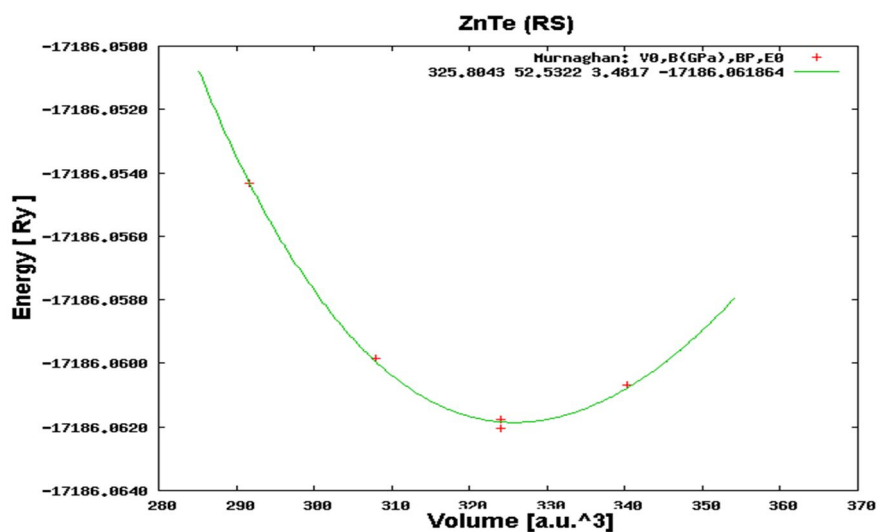

Figure 2: Energy vs volume for ZnTe in rocksalt structure.

Table I.: Calculated equilibrium lattice constants (a_0), bulk modulus B_0, and the pressure derivative of bulk modulus (B_0') along with related experimental data and the other theoretical works for ZnTe in ZB and RS phases.

ZnTe	Calculations	a_0 (Å)	B_0 (GPa)	B_0'
ZB phase	Present work	6.18	51.46	3.06
	Theory [Ref.24]	6.02	49.2	-
	Theory [Ref.25]	6.18	49.8	4.78
	Exp.[Ref.26]	6.08	50.9	-
	Exp.[Ref.27]	6.10	50.9	-
RS phase	Present work	5.78	52.53	3.48
	Theory [Ref.28]	5.50	45.98	5.62

It can also noted that the lattice constant of ZnTe found to be reduced at high pressure whereas bulk modulus is found to be increased with increase in pressure and derivative of bulk modulus ($\mathbf{B_0'}$) is also increased with pressure.

B. Optical Properties

The optical properties of a matter can be described by the complex dielectric function (ω), which represents the linear response of the system to an external electromagnetic field with a small wave vector. First of all, the imaginary part of dielectric tensor is computed from the electronic band structure of ZnTe solid. Further, the real part of the dielectric function is extracted from the imaginary part using the Kramers-Kronig relations [29]. And finally, the other optical properties (like absorption coefficient, optical conductivity, refractive index etc.) of the cubic ZnTe in zinc blende(B3) and rock salt(B1) phases have been investigated in terms of the imaginary and real parts of complex dielectric function. From the Figure 3, it is noted that the $\varepsilon_2(\omega)$ shows a large peak (located at 4.25 eV for ZnTe between two small peaks for the ZB phase.
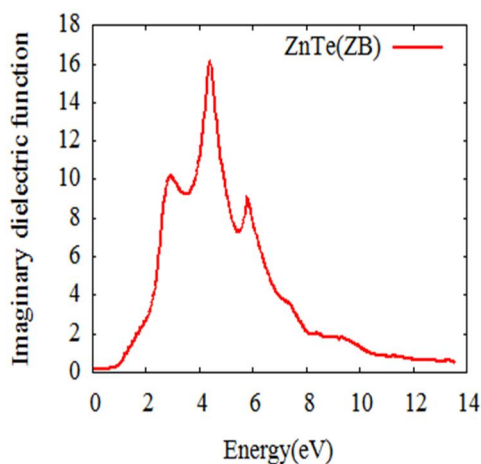

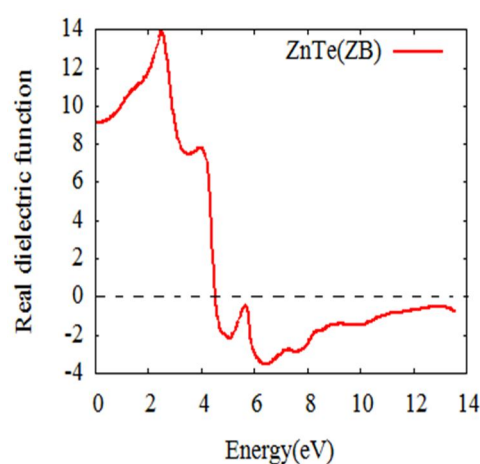Fig. 3.: Imaginary dielectric function $\varepsilon_2(\omega)$ of ZnTe(ZB).

Fig. 4: Real dielectric function $\varepsilon_1(\omega)$ of ZnTe(ZB).

Moreover, another observation of the Figures 3 and 5 that all the peaks structures in $\varepsilon_2(\omega)$ are shifted a little towards the lower energies with increase in the peak heights in case of RS phase under high pressure. Overall good agreements have been found with the theoretical and experimental data [30-32] with reference to the peaks position and peak heights. The results of calculated real dielectric function $\varepsilon_1(\omega)$ for ZnTe compound in ZB phase is shown in the Figure 4. It is noticed that a smaller energy gap yields a

larger $\varepsilon_1(0)$ value. It could be explained on the basis of the Penn model [33]. Further, the results are compared with the experimental data [32] available, good agreements have been found.
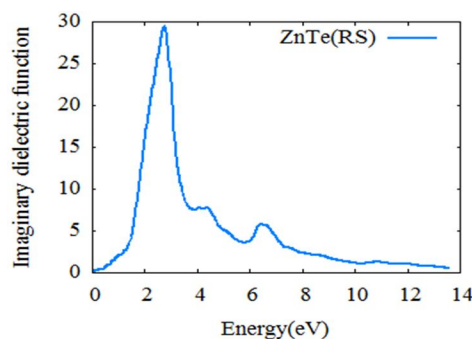

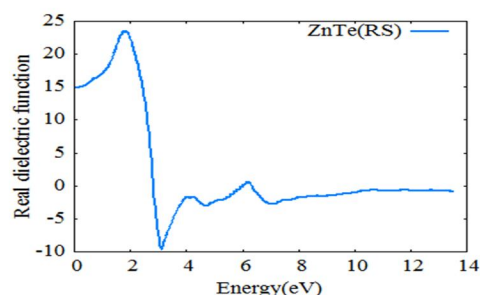Fig. 5: Imaginary dielectric function $\varepsilon_2(\omega)$ of ZnTe(RS).

Fig. 6: Real dielectric function $\varepsilon_1(\omega)$ of ZnTe(RS).

The Figure 5 shows the calculated imaginary dielectric function $\varepsilon_2(\omega)$ for the ZnTe compounds in RS phase. This may be noted that the $\varepsilon_2(\omega)$ shows a large peak (located at 2.9 eV) for ZnTe RS phase. The results of the calculated real dielectric function $\varepsilon_1(\omega)$ for ZnTe compound in RS phase are shown in the Figure 6. The calculated static dielectric constants $\varepsilon_1(0)$ are presented in the Table II for both ZB and RS phases of ZnTe .

Table II: Calculated static dielectric constant for cubic ZB and RS phases of ZnTe.

ZnTe	Calculations	Static dielectric constant , $\varepsilon_1(0)$
ZB Phase	Present work	9.2
	Theory[Ref.30]	5.24
	Theory[Ref.34]	8.1
	Exp.[Ref.35]	7.3
	Exp.[Ref.36]	7.3
RS Phase	Present work	6.0
	Others	-

The Figure 7 shows the calculated absorption spectrum $\alpha(\omega)$, for the ZnTe compound in ZB phase. It may be noted that the the absorption edge start from about 0.26 eV for ZnTe corresponding to the direct Γ-Γ transition.

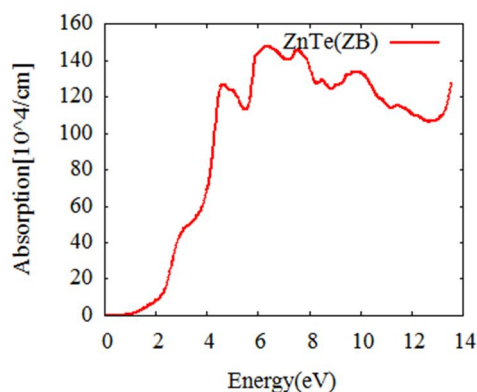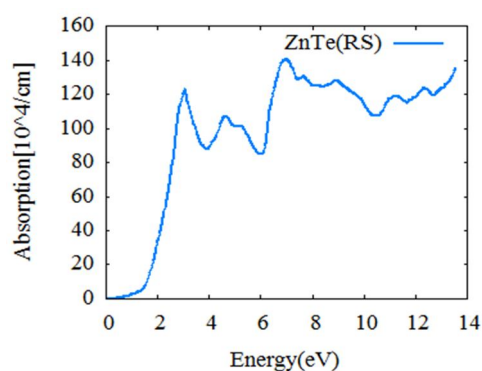

Fig.7: Absorption $\alpha(\omega)$ of ZnTe(ZB).

Fig. 8: Absorption $\alpha(\omega)$ of ZnTe(RS).

The absorption spectrum $\alpha(\omega)$, shows a very intense absorption, which occurs at around 4.52 eV for ZnTe due to excitations of photons. The shown results are found similar to the experimental findings reported earlier [37] in case of peaks position and height. The Figure 8 shows the calculated absorption spectrum $\alpha(\omega)$ for the ZnTe compound in RS phase. It is observed that the absorption edge start from about 0.20 eV for ZnTe and reached at maximum peak around 7.1 eV corresponding to the transitions from different symmetry directions.

The occupied electron states are excited to unoccupied electron states in upper Fermi level by absorbing photons. This interband transition is also called Drude transition and photon absorption by electron is called interband absorption. This may also be called as internal photoelectric effect. As in the Figure 9, the optical conduction starts with energy of about 0.20 eV for ZnTe in the ZB phase and by increasing photon energy, the optical conduction rises and reached at maximum.
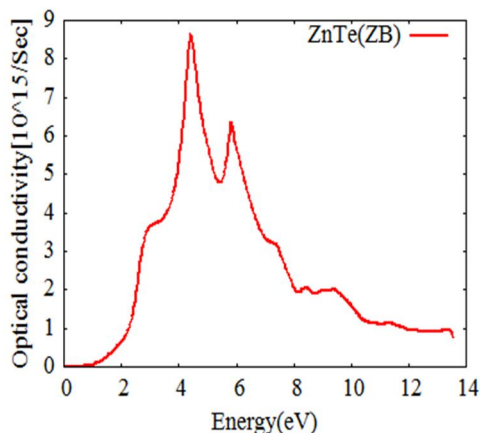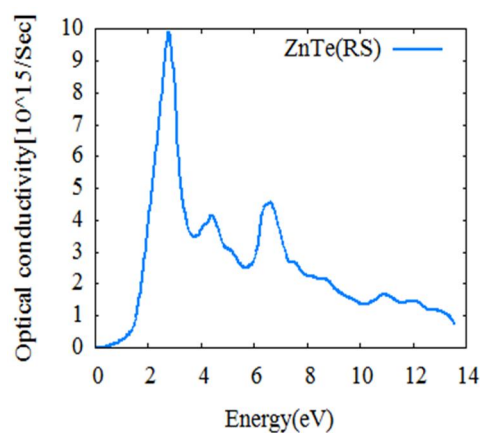

Fig. 9: Optical conduction of ZnTe(ZB).

Fig. 10: Optical conduction of ZnTe(RS).

The reason of starting optical conduction $\sigma(\omega)$, from above said energy range, is the gap of energy between valence and conduction band at Fermi level. As the excited electrons have no enough energy to pass the energy gap, and transfer to the conduction band in case of lower energy side and thus have weak signal. Our results obtained are similar to the experimental findings reported earlier [49] in case of peaks position and height. The Figure 10 shows that the optical conduction $\sigma(\omega)$ starts with energy of about 0.19 eV for ZnTe in the RS phase and by increasing photon energy, the optical conduction is rised and then reached at maximum. The further increase of the energy results a decrease in optical conduction. This decrease in conductivity signal may probably be interepted due to the fact that the interaction increases with electron density and thus resistance increases. It is also observed that all the structures in $\sigma(\omega)$, are shifted a little towards the lower energies with increase in the peak heights as compared to Figure 9. The Figure 11 represents the refractive index spectra for the ZnTe compound in ZB phase. This shows that the refractive index is significant only upto of 2.4 eV for ZnTe beyond this energy value it drops sharply.
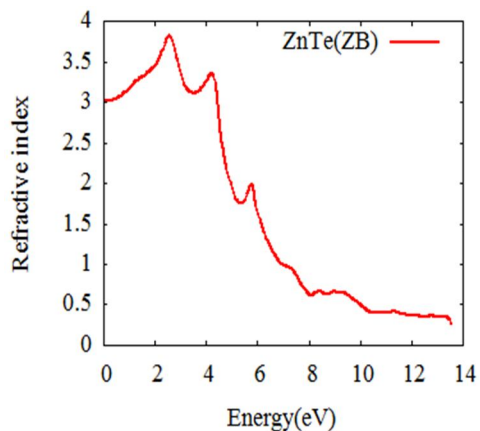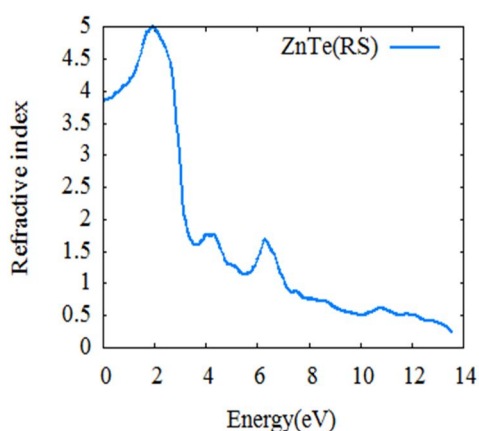

Fig. 11: Refractive index of ZnTe(ZB).

Fig. 12: Refractive index of ZnTe(RS).

The theoretically calculated static refractive index 3.01 for ZB ZnTe is displayed in Table III. The Figure 12 represents the refractive index spectra for the ZnTe compound in RS phase. This shows that the refractive index is significant only upto 2.1 eV for ZnTe and beyond this energy value it drops sharply. Our theoretically calculated static refractive index is found 3.84 for ZnTe for RS phase as written in the Table III. However, there is no experimental data available of ZB and RS phase in the literature, so comparison could not be possible.

Table III: Calculated static refractive index for cubic ZB and RS phases of ZnTe.

ZnTe	Calculations	Static refractive index $n(0)$
ZB Phase	Present work	3.01
	Others	-
RS Phase	Present work	3.84
	Others	-

The electron energy loss function $L(\omega)$, is a significant factor related to the energy loss of fast electrons traversing in the material. The EELS is a valuable tool for investigating various properties of such materials. In Figure 13, the most prominent peak in the energy loss spectrum is connected with the Plasmon peak and located at 13.12 eV for ZnTe in the ZB phase and the resultant frequency is called plasma frequency ($\hbar\omega_p$) [38].
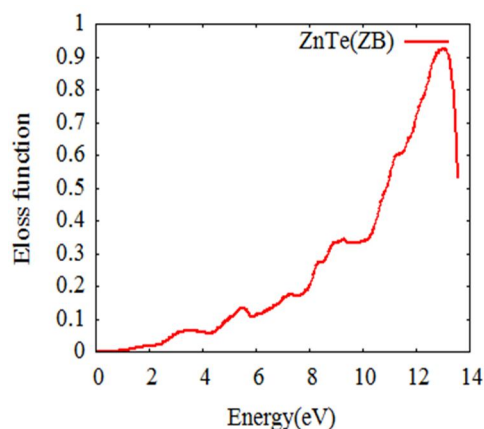

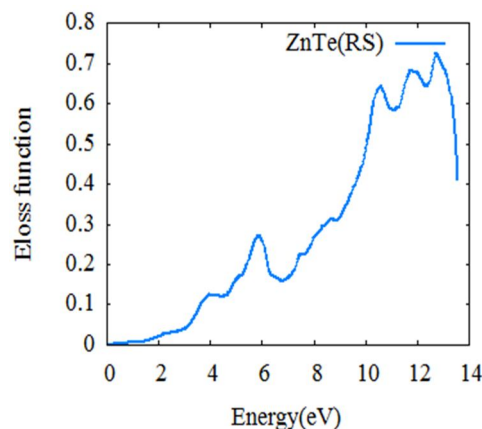Fig. 13: Eloss function of ZnTe(ZB).   Fig. 14: Eloss function of ZnTe(RS).

Further, in the second case of RS phase of ZnTe, the Figure 14 represents the most prominent peak in the energy loss spectrum associated with the plasmon peak and located at 12.99 eV. The plasmon energy value ($\hbar\omega_p$) obtained in this work for ZB and RS phases are given in Table IV.

Table IV:. The plasmon energy $\hbar\omega_p$ of the energy loss function for the ZnTe in ZB and RS phases.

ZnTe	$\hbar\omega_p$ (eV)
ZB-phase	13.12
RS-phase	12.99

The extinction coefficient $k(\omega)$ is calculated and presented in the Figure 15 and 16 of ZnTe in ZB and RS phases. The local maxima of the extinction coefficient $k(\omega)$ corresponds to the zero of $\varepsilon_1(\omega)$ (4.90 eV) for ZnTe in ZB phase and 2.89 eV for ZnTe in RS phase, respectively.
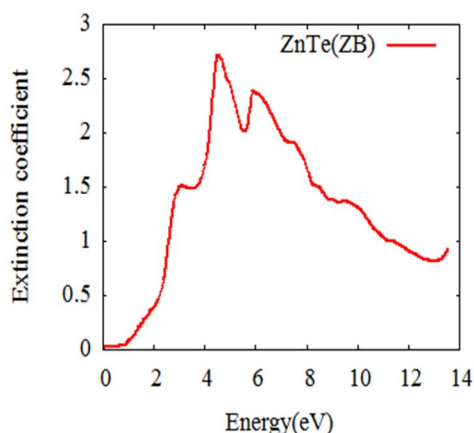
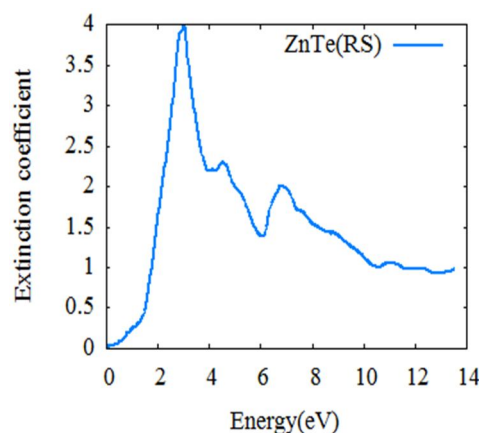Fig. 15: Extinction coefficient of ZnTe(ZB).   Fig. 16: Extinction coefficient of ZnTe(RS).

The results are found similar to the experimental findings reported earlier [37] with regard to peaks position and height for ZB structure. There is no experimental data available for of RS phase in the literature, so comparison is not possible. But our computed result may be very useful for further experimental and theoretical study of high pressure RS phase.

IV. CONCLUSIONS

We have performed calculations of the structural parameters and optical response for the ZnTe compounds, using FP-LAPW methods. The calculated lattice constant and bulk modulus are found in good agreement with the available experimental data. All the peak structures in the imaginary part of the dielectric function $\varepsilon_2(\omega)$ are shifted towards lower energies for ZB and RS phases of ZnTe. The obtained results of imaginary dielectric function $\varepsilon_2(\omega)$ have been compared with the earlier reported experimentally measured frequency dependent dielectric function and previous theoretically calculated values. Overall well agreements have been found. We have also found that the theoretically obtained values of static dielectric constant $\varepsilon_1(0)$ and static refractive index increases with decreasing energy gap which are in well agreement with the Penn model. The same trend has been found in the case of RS phase. Further, We have also calculated the other optical properties like absorption, optical conductivity, eloss function and extinction coefficient spectra for ZB and RS phases of ZnTe compound seeking for more detail comparison with the earlier reported experimental results.

REFERENCES

[1] K. J. Chang, S.1oyen and M.L. Cohen, Solid State Commun. 50 (1984) 105.

[2] R. Laihia, J. A. Leiro, K. Kokko and Mansikka, Journal of physics Condensed Matter 8 (1996) 6791-6801.

[3] Landolt-Bornstein Numerical Data and Functional Relarionship in Science and Technology, New Series, Vol. 17b (1982).

[4] K. Shahzad, D. J. Olego and C.G. Van de Walle, Phys. Rev. B 38 (1998) 1417.

[5] I. Gorczyca and N.E. Christensen, Solid State Commun. 72 (1989) 785.

[6] N. E. Christensen. I. Gorcyca, O.B. Christensen U. Schmid and M. Cardona, J. Crystal Growth 101 (1990) 318.

[7] I. H. Shan, I. Inoue, O. Matsuda, K. Murase, T. Yokogawa and M. Ogura, Solid State Commun 67 (1998) 779.

[8] S. Ves. K. Strossner, N.E. Christensen, C.K. Kim and M. Cardona, Solid State Commun. 56 (1985) 479.

[9] K. Strossner, S.Ves, C.K. Kim and M. Cardona, Solid State Commun. 61 (1987) 2755.

[10] S. R. Tiong, M. Hiramatsu, Y. Matsushima and E. Ito, Jpn. J. Appl. Phys. 28 (1989) 291.

[11] M. Bilge, S. Ozdemir Kart, H. H Kart and T. Caging, Journal of Achievement in Materials and Manufacturing Engineering, 31(2008)29.

[12] P. Blaha and K. Schwarz, WIEN2k, Vienna University of Technology Austria, 2009.

[13] G. H. K. Madsen, P. Blaha, K. Schwarz, E. Sjöstedt and L. Nordström, Phys. Rev. B 64, 195134-1(2001).

[14] P. Dufek, P. Blaha, K. Schwarz, Phys.Rhys. Rev. B 50(1994)7279.

[15] G.H.K. Madsen, B.B. Iversen, P. Blaha and K. Schwarz, Phys. Rev. B 64 (2001) 195102-1-6.

[16] D. D. Koelling and B.N. Harmon, J. Phys. C 10 (1977) 3107.

[17] J. P. Perdew, J. A. Chevary, S. H. Vosko, K. A. Jackson, M. R. Pederson, D. J. Singh and C. Fiolhais, Phys. Rev. B Vol. 46 (1992) 6671-6687.

[18] M. Peterson, F. Wanger, L. Hufnagel, M. Scheffler, P.Blaha and K. Schwarz, Computer Physics Communications 126 (2000) 294-309.

[19] K. Schwarz, J. Sol. St. Chem. 176 (2003) 319.

[20] K. Schwarz and P. Blaha, Comput. Mat. Sci. 28 (2003) 259.

[21] K. Schwarz, P. Blaha and G. K. H. Madsen, Comput. Phys. Commun. 147 (2002) 71.

[22] M. Peterson et al., Comput. Phys. Commun., 126 (2000) 294.

[23] F. D. Murnaghan, Proc. Natl. Acad. Sci. USA,30 (1944) 244.

[24] S. H. Wei, A. Zunger, Phys. Rev. B 37 (1988) 8958.

[25] N. E. Christensen and O. B.Christensen, Phys. Rev. B 33(1986)4739.

[26] O. Madelung, Numerical Data and Functional Relationships in Science and Technology, New Series, Vol.17b (Springer-Verlag, Berlin, 1982).

[27] Numerical Data and Functional Relationship in Science and Technology, edited by O. Madelung, M. Schulz, and H. Weiss, Landolt-Brnstein, New Series, Group III _Springer-Verlag, Berlin, Vol. 17a(1982) 159.

[28] S. Denilson. Borges and J. P. Rino, Phys. Rev. B 72 (2005) 014107.

[29] P.Y. Yu, M. Cardona, Fundamentals of Semiconductors Physics and Materials Properties , Springer-Verlag, Berlin(1999)233.

[30] M. Z. Huang and W.Y. Ching, Phys. Rev. B 47, 9449 (1993); Phys. Rev. B 47 (1993) 9464.

[31] E. Ghahramani, D. J. Moss, and J. E. Sipe, Phys. Rev. B 43 (1991) 9700; 43 (1991) 8990.

[32] J. L.Freeouf, Phys. Rev. B 7 (1973) 3810.

[33] D. R. Penn, Phys. Rev. 128 (1962) 2093.

[34] A. Dal Corso, F. Mauri, and A. Rubio, Phys. Rev. B 53 (1996) 15638.

[35] D. E. Aspnes, Phys. Rev. B 6 (1972) 4648.

[36] N. Vagelatos, D. Wehe and J. S. King, J.Chem.Phys. 60 (1974) 3613.

[37] Optical Constants of Crystalline and Amorphous Semiconductors: Numerical data and Graphical information, edited by S. Adachi (Kluwer Academic, Boston, 1999).

[38] P. Nozieres, Phys.Rev. Lett. 8(1959)1.

INTERNATIONAL JOURNAL FOR RESEARCH

IN APPLIED SCIENCE & ENGINEERING TECHNOLOGY

Call : 08813907089 ⓒ (24*7 Support on Whatsapp)